Ab initio MOLECULAR DYNAMICS FOR DETERMINATION OF STRUCTURES OF ALKALI METAL CLUSTERS AND THEIR TEMPERATURES BEHAVIOR; AN EXAMPLE OF Li_9^+

Vlasta BONACIC-KOUTECKY[a1], Detlef REICHARDT[a2], Jiri PITTNER[a3,*], Piercarlo FANTUCCI[b] and Jaroslav KOUTECKY[c]

[a] *Humboldt-Universitat zu Berlin, Walther-Nernst-Institut fur Physikalische und Theoretische Chemie, Bunsenstrasse 1, 10117 Berlin, Germany; e-mail: [1] vbk@kirk.chemie.hu-berlin.de, [2] detlef@kirk.chemie.hu-berlin.de, [3] jiri.pittner@jh-inst.cas.cz*

[b] *Dipartimento di Chimica Inorganica, Metallorganica e Analitica, Centro CNR, Universita di Milano, Via Venezian 21, 20133 Milano, Italy; e-mail: fant@inorg141.csmtbo.mi.cnr.it*

[c] *Freie Universitat Berlin, Institut fur Physikalische und Theoretische Chemie, Takustrasse 3, 14195 Berlin, Germany; e-mail : jk@kirk.chemie.hu-berlin.de*

Received June 30, 1998
Accepted July 9, 1998

Dedicated to Professor Rudolf Zahradnik on the occasion of his 70th birthday.

It will be shown that an *ab initio* molecular dynamics procedure based on gradient corrected density functionals for exchange and correlation and using a Gaussian atomic basis (AIMD-GDF) implemented for parallel processing represents a suitable tool for detailed and accurate investigation of structural and dynamical properties of small systems. Gradients of the Born–Oppenheimer ground state energy, obtained by iterative solution of the Kohn–Sham equations, are used to calculate the forces acting on atoms at each instantaneous configuration along trajectories generated by solving classical equations of motion. Dynamics of different isomers of the Li_9^+ cluster have been investigated as a function of excess energy. It is shown that different isomers, even those similar in energy, can exhibit different structural and dynamical behavior. The analysis of the simulations leads to the conclusion that structures with a central atom, in particular the centered antiprism of Li_9^+ exhibit concerted mobility of the peripheral atoms at relatively low excess energy. In contrast, compact tetrahedral type structures show much more rigid behavior at low excess energy. However, the former ones need larger excess of internal energy to undergo isomerizations to geometrically different structures than the latter ones. At the time scale of our simulations we found that for the intermediate excess energies it is "easier" to carry the cluster in the basin of the lowest energy isomer than in the reverse direction. It has been found that the liquid-like behavior in small Li clusters becomes apparent at relatively high temperature in spite of large mobility of their atoms.

Key words: *Ab initio* molecular dynamics; Density functional; Alkali metal clusters; Lithium; *Ab initio* calculations.

* Permanent address: J. Heyrovsky Institute of Physical Chemistry, Academy of Sciences of the Czech Republic, 182 23 Prague 8, Czech Republic.

The importance of small atomic clusters has received increasingly recognition due to evidence that novel physical and chemical phenomena can be obtained by controlling the cluster size, shape and temperature[1]. The extrapolation from the bulk properties towards the atom[2] proved to be inadequate, since it does not account for individual characteristics of the given cluster size, which play a key role in determining electronic and structural properties. New areas of applications such the construction of quantum dot lasers or single electron transistors, although still in a development stage[1,3], have confirmed this fact. In spite of many open questions concerning the success of constructing such devices, it is now clear, that the addition of a single atom or a few atoms to a given cluster can be the way of modulating the color of emitted light which, in addition, will further depend on the nature of the atoms. Similarly, a significant effect on the transport properties has been found studying the rearrangements of atoms in sodium nanowires which can be influenced by elongating the wire (changing the temperature)[4]. These nanowires assume molecular type supported structures related to the known shapes of the gas phase sodium clusters[5].

The need for the precise determination of structural, optical and dynamical properties of small pure and mixed metal clusters based on *ab initio* quantum chemical treatments[6–8] has been widely recognized. In fact the *ab initio* studies provided precise data on structures and stabilities of neutral and charged alkali metal clusters well before the experimental setups reached the accuracy[9–12] which could make use of these results. A direct experimental evidence of the ground state geometries of small metal clusters in the gas phase is still not available, but spectroscopic techniques[13–16] can probe the size-dependent structural properties *via* the cluster excited states. These findings are relevant, however, provided that a complementary theoretical information is available. In fact, the *ab initio* determination of optically allowed transitions and their intensities for the stable cluster structures has been established as a reliable predictive tool, particularly for simple metals[17–20] or mixed aggregates[21]. A comparison of *ab initio* spectroscopic patterns[17–21] with experimental data allowed in several cases to assign the measured features to a specific cluster structure.

Such a comparison is strictly valid at zero temperature. Depletion spectra of alkali metal clusters have been recorded first at relatively high temperatures[13,14,22,23], while only more recently low temperature data[16] as well as spectra obtained by two photon femtosecond spectroscopy[15] became available. However, the presence of energetically close lying isomeric forms corresponding to local minima and separated by low barriers is typical for small pure and mixed metallic clusters. Therefore, it might be necessary to consider the contributions of different isomeric forms when simulating the experimental optical spectra recorded at low or moderate temperature.

The ground state *ab initio* molecular dynamic is particularly useful to study influence of the temperature on structural properties, allowing to determine the statistical import-

ance of individual isomers at the given temperature as well as the mechanism of isomerization process[24–28].

In this paper we will first briefly outline the *ab initio* molecular dynamics method which we developed mainly with the aim of studying temperature dependent ground state properties. Then, the results of *ab initio* molecular dynamics (AIMD) of Li_9^+ will be presented as an example of a different temperature behavior of different cluster structures. The investigation of isomerization processes will also allow to formulate precise criteria for "phase transition" from solid-like to liquid-like behavior for finite systems.

Ab initio MOLECULAR DYNAMICS FOR DETERMINATION OF STRUCTURES OF ALKALI METAL CLUSTERS AND THEIR TEMPERATURES BEHAVIOR

Ab initio molecular dynamics (AIMD) which couples quantum mechanical treatment of electrons and forces acting on nuclei with classical equations of motions[29,30] has been established as a powerful method for search of geometries corresponding to local minima on energy surfaces. The advantage of the AIMD over the conventional gradient based geometry optimization is that all local minima can be in principle accessed. Namely, the cluster geometries generated along the classical trajectories can be used for search of isomeric forms on the energy potential surfaces. The accurate determination of the electronic energies and forces can be achieved either at the Hartree–Fock[31,24–26] (HF) or density function level employing Gaussian basis sets[27,28] (GDF). Both procedures allow therefore, the identification of stable isomers and, in addition, the investigation of dynamical and temperature behavior.

The idea of AIMD, originally initiated by Car and Parrinello[29] in connection with a DF procedure employing a plane waves expansion, is here revisited in terms of a quantum chemical approach based on fully self consistent energies and gradients in the framework of the HF (refs[24–26]) or GDF (refs[27,28]) procedures, employing the AO basis sets centered at the nuclei.

The classical trajectories are calculated using the Verlet algorithm (*cf.* ref.[24]) according to which the position and velocity of the nucleus i ($\boldsymbol{r}_i$, $\boldsymbol{v}_i$) at time step $t_n = n\Delta t$, are obtained recurrently:

$$\boldsymbol{r}_i^{(n+1)} = 2\boldsymbol{r}_i^{(n)} - \boldsymbol{r}_i^{(n-1)} + \frac{\Delta t^2}{m}\boldsymbol{F}_i^{(n)} \qquad (1)$$

$$\boldsymbol{v}_i^{(n+1)} = \boldsymbol{v}_i^{(n)} + \frac{\Delta t}{m}(\boldsymbol{F}_i^{(n-1)} + \boldsymbol{F}_i^{(n)}) \ . \qquad (2)$$

The force $\boldsymbol{F}_i^{(n)}$ acting on nucleus i is related to the gradients of the total molecular energy computed at SCF (HF or DF) level. The ground state electronic wavefunction

and energy are computed at each time step (*i.e.* for each geometric configuration). In our AIMD-HF or AIMD-DF programs the total molecular energy obtained from iterative HF or iterative Kohn–Sham procedure, is the potential energy and its corresponding derivatives are the forces acting on the nuclei.

The accuracy of calculated energies and gradients must be higher than usually needed for the geometry optimization, since the precise determination of forces is required for the conservation of the total energy. In order to obtain meaningful information on dynamical properties sufficiently long trajectories have to be calculated. The computational demand is large due to both requirements. Therefore, different strategies had to be used to speed up calculations. Since both AIMD-HF and AIMD-DF schemes are suitable for parallel processing, the efficiency of the programs has been achieved first by means of a full parallelization of the most numerically demanding algorithms. Secondly, all input–output operations have been eliminated by keeping the integrals in memory and finally, a careful optimization of the sequential parts has been introduced[25,28]. However, applications are limited to small systems, particularly in the case of AIMD-DF with gradient corrections owing to time-consuming numerical three-dimension integration of the functionals for the exchange-correlation (*e.g.* those proposed by Becke[32] and Lee, Yang and Parr[33] (B-LYP)).

In spite of these limitations AIMD schemes represent suitable tools to study not only structural features but also the influence of internal energy on the dynamics of metal clusters. The latter aspect is particularly important, since it allows to investigate mechanism of isomerization processes with increasing temperature[24–28]. For this purpose the trajectories need to be calculated over a broad range of different fixed total energies. The total energy of a cluster is varied by random distortions of its equilibrium geometry in the case that zero initial atomic velocities are assumed. We have chosen initial conditions which satisfy the requirement of zero linear and angular momenta of the clusters. The time step is equal to 0.5 fs and the lengths of the simulations range from 10 to 40 ps. The conservation of the total cluster energy in the longest runs was better than 10^{-2} eV, due to the high-accuracy criteria for calculations of energies and derivatives.

A small split valence basis set with three s-functions and one p-function was used in our AIMD calculations[24–28]. Cluster geometries, which were generated along the trajectories at high internal energies were employed as initial coordinates in a gradient-based search for stable isomers, which were identified as local minima by carrying out a full harmonic vibrational analysis. In addition to the isomers already found by standard optimization techniques[6–12] the AIMD procedure gave evidence of existence of other isomeric forms. The structures and energy sequence of the isomers of Li_n clusters obtained using a small AO basis were in agreement with the corresponding results obtained with considerably larger basis sets[10].

The long time average of the kinetic energy $\langle E_k \rangle$ over the entire length of a trajectory was used to estimate the temperature T of a cluster according to $T = 2\langle E_k \rangle/(3n - 6)k$,

where n is the number of atoms and k is the Boltzmann constant[24–28]. The influence of internal energy (temperature) on dynamics of Li_9^+ cluster obtained in the framework of a gradient corrected AIMD-DF approach (B-LYP) will be presented in the next section.

RESULTS AND DISCUSSION OF DYNAMICS OF Li_9^+ CLUSTER

In a previous work on structural properties, the centered antiprism (D_{4d}) has been identified as the most stable isomer of Li_9^+ at the HF level[9] (isomer **1**). This result was confirmed also by an electron correlation treatment using large scale CI (refs[6,10]) as well as by the geometry optimization with the gradient corrected density functional method (B-LYP). However, two other isomeric forms close in energy have been found by standard geometry optimization techniques as well as by AIMD schemes: the C_{2v} structure (isomer **2**) (which can be obtained by capping the T_d form of octamer or by bicapping a pentagonal bipyramid) and the C_{3v} form (isomer **3**) (a deformed section of the fcc lattice). They were identified as local minima by harmonic frequency analysis, both in the framework of the HF and B-LYP procedure. At the HF level, the energy sequence is $D_{4d} < C_{2v}(\Delta E = 0.06$ eV) $< C_{3v}(\Delta E = 0.20$ eV). The electron correlation effects included in the density functional treatment increase the energy separation of the isomers **2** and **3** with respect to the isomer **1** ($\Delta E = 0.22$ and $\Delta E = 0.40$ eV) but the energy sequence remains unchanged[34].

We have chosen to discuss temperature behavior of individual isomers of Li_9^+ cluster because they are characterized by distinct type of structures. Note that the most stable isomer of Li_9^+ (D_{4d}) assumes a shape different from the most stable isomer of Na_9^+ (C_{2v}). Therefore distinct temperature behavior of Li_9^+ and Na_9^+ clusters might be expected. Investigation of the temperature behavior of the neutral Na_n cluster has been carried out using Car, Parrinello method[29] employing DF with gradient corrections and plane waves[35]. Notice that gradient corrections introduced in DF by Becke[32] for exchange part of the functional, which improved the determination of binding energy and bond distances considerably, proved to be also very important for calculation of the energy sequences of the isomers.

Our simulations were initialized from randomly distorted geometries of different isomers of Li_9^+, and zero initial velocities (*cf.* the preceding section and refs[24–28]). The results obtained from AIMD-B-LYP simulations will be analyzed[34] using the following four quantities. We find particularly instructive to analyze the trajectories in terms of "atomic equivalence indeces"

$$\sigma_i(t) = \sum_i | \boldsymbol{r}_i(t) - \boldsymbol{r}_j(t) | \ , \qquad (3)$$

where $\boldsymbol{r}_i(t)$ is the position of the atom i at the time t (ref.[26]). The $\sigma_i(t)$ quantities account for all the structural information for a given atom, which depends on the position of all

the surrounding atoms at the given time. The non-accidental degeneracies of the $\sigma_i(t)$ quantity reflect also the symmetry equivalence of a subset of atoms. Structures which do not coincide with a local minimum but belong to its basin of attraction are characterized by $\sigma_i(t)$ values which are "similar" to those of the isomer. Sharp variations in $\sigma_i(t)$ values along a trajectory indicate transition from one to another basin and therefore an isomerization process. Moreover, $\sigma_i(t)$ curves allow the identification of the atomistic mechanism of an isomerization and to distinguish between pathways characterized by concerted motion of atoms from those along which exchange between atoms occurs. Also at relatively high internal energy (temperature) the analysis in terms of $\sigma_i(t)$ quantities is helpful, since one can easily identify the time intervals connected with different isomers.

The root-mean-square (RMS) bond length fluctuation δ (ref.[24]), which is calculated at the end of trajectories, has been often used for bulk materials. A sharp increase of the δ value is known as the Lindemann criterion for bulk melting, while in the context of finite-size clusters it has been taken as an indication of transition from solid-like to liquid-like state. However, large atomic displacements can occur which are not representative of isomerization processes but which cause increase in δ values. Therefore, the transition from solid-to liquid-like state cannot be determined only on the basis of δ quantities for small finite systems.

Additional information about the dynamical behavior of a cluster associated with a local structure can be obtained from the power spectrum defined as

$$f(\omega) = \int_0^t \frac{\langle \boldsymbol{v}(t)\boldsymbol{v}(0)\rangle}{\langle \boldsymbol{v}(0)\boldsymbol{v}(0)\rangle} \cos(\omega t)\, \mathrm{d}t \ , \qquad (4)$$

which is the Fourier transform of the velocity autocorrelation function defined as

$$\langle \boldsymbol{v}(t)\boldsymbol{v}(0)\rangle = \frac{1}{n n_t} \sum_{j=1}^{n_t} \sum_{i=1}^{n} \boldsymbol{v}_i(t_{0j} + t)\ \boldsymbol{v}_i(t_{0j}) \ . \qquad (5)$$

In Eq. (5), n_t is the number of time origins t_{0j}.

The analysis of trajectories in terms of $\sigma_i(t)$ quantities, the power spectra, short-time averaged kinetic energy per atom $\langle E_k/n\rangle$ and bond length fluctuations δ are presented on Figs 1–5.

The plots of $\sigma_i(t)$ values at low internal energy (temperature) along trajectories initialized from the three isomers D_{4d}, C_{2v} and C_{3v} of the Li_9^+ cluster are shown in Fig. 1 and serve as a guidance for identification of groups of equivalent atoms with (almost) degenerate $\sigma_i(t)$ values. For the same trajectories the calculated power spectra are shown on the right hand side of Fig. 1. The comparison of power spectra obtained at low excess energy for all three isomers is instructive because different features can be

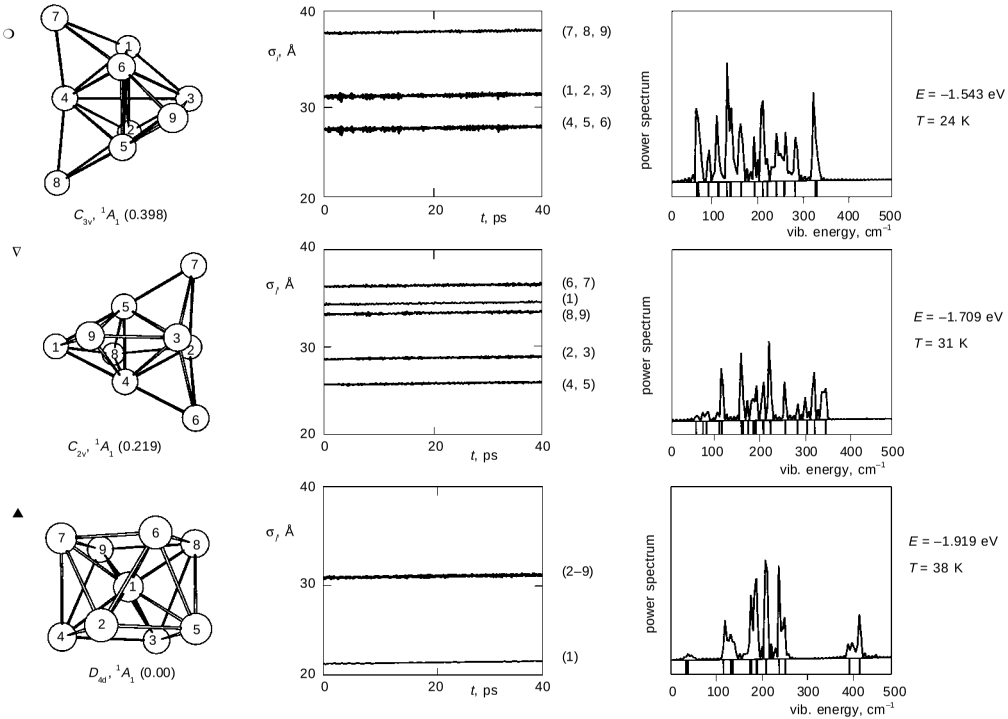

FIG. 1

Short-time (0.25 ps) averaged "atomic equivalence indexes" $\sigma_i(t)$ (Å) as functions of time for trajectories of Li_9^+ cluster initialized from (i) a distorted D_{4d} structure (isomer **1**, ▲) with the fixed total energy of –1 830.919 eV; (ii) a distorted C_{2v} structure (isomer **2**, ∇) with the total energy of –1 830.709 eV; (iii) a distorted C_{3v} structure (isomer **3**, ❍) with the total energy –1 830.543 eV. Nearly equivalent atoms are grouped in parenthesis on the right side of windows in accordance with the numbering of atoms of the corresponding structures of the isomers drawn on the left side. The relative energy sequence of the isomers obtained from B-LYP procedure is given. Power spectra (evaluated for the corresponding trajectories of the left hand side) obtained by Fourier transform of the velocity autocorrelation functions are shown at the right side. Frequencies calculated by harmonic analysis of the given isomeric form are indicated by vertical lines[34]

identified. The positions of peaks correspond to frequencies obtained by harmonic vibrational analysis (vertical lines), whereas the intensities are dependent on the particular run. The power spectrum related to the D_{4d} is characterized by peaks located at ≈100, 200–350 cm^{-1} and a particularly narrow peak at ≈400 cm^{-1}. The latter one is absent in the power spectra of isomers of C_{2v} and C_{3v} symmetry, which are characterized by peaks spread in the interval between 100 and 300 cm^{-1}.

The difference in dynamical behavior of three isomers investigated at different cluster energies (temperature) can be clearly seen from Figs 2–5.

From the graphs of $\langle E_k/n \rangle$ resulting from trajectories initiated from a distorted centered antiprism (isomer **1**) shown in Fig. 2, it is possible to see that the fluctuations are present already at T = 182 K and become larger with increasing temperature. This is even more evident from the analysis in terms of $\sigma_i(t)$ quantities, as shown on the right side of Fig. 2. The pheripheral atoms of the centered antiprism (2–9) (see Fig. 1 for patterns of reference $\sigma_i(t)$) are highly mobile but no exchange occurs with the central atom (1), which is characterized by low σ_i value, until $T \approx 472$ K. The sudden change of $\sigma_i(t)$ value for the central atom indicating its exchange with one of the pheripheral atoms occurs first at $T \approx 513$ K. At this temperature (internal energy) the mechanism responsible for the isomerization can be followed, which is reflected in a sudden change of the values of $\sigma_i(t)$ which now are those characteristic for the structures of isomers **2** and **3** (*cf.* Fig. 1). This is in agreement with the results obtained by the gradient based quenching procedure applied to the trajectory of the graph 2Ac (T = 513 K). The graph 2Be (T = 513 K) is particularly instructive since it shows that the liquid stage of Li_9^+ has not been reached yet at a temperature higher than 500 K.

The peripheral atoms of the centered antiprism perform a concerted type of motion leading to equivalent isomeric forms of **1**. The atomistic mechanism can be visualized as a concerted mutual rotation of two opposite square faces of the antiprism accompanied by relaxation of the interplane distance. For an idealized case of a cubooctahedron, the atoms belonging to two parallel faces (identified by labels of Fig. 1 collected in parenthesis) (2345)/(6789) rearrange into an equivalent form *e.g.* (2467)/(3589) by two successive rotations of one face with respect to the other by 45° in opposite directions. The first rotation, which would bring the D_{4d} structure into the D_{4h} one, has never been identified, since the concerted motion of all eight atoms occurs avoiding always the more symmetrical D_{4h} structure which lies in energy 0.15 eV above the D_{4d} one. The concerted motion defines a possible path between two equivalent forms along which a saddle point has been found with the energy of 0.007 eV above the D_{4d} form. Notice that the exact determination of the saddle point is very difficult on such an flat energy surface. The concerted motion of peripheral atoms of the centered antiprism leading to equivalent isomeric forms is a relatively slow process at low excess of internal energy occurring on a time scale of a few picoseconds for the trajectory of the graph 2Aa (T = 182 K).

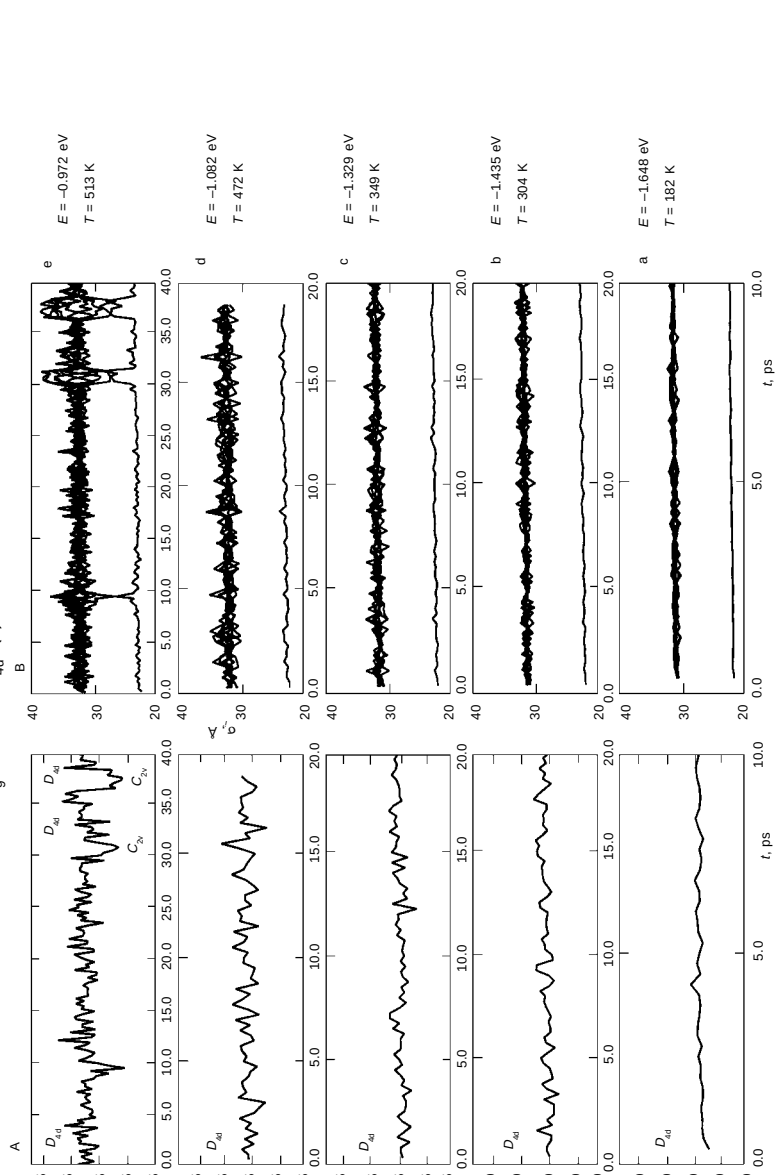

FIG. 2
Short-time (0.25 ps) averaged kinetic energy per atom ⟨KE⟩ (A) and "atomic equivalence indexes" $\sigma_i(t)$ (B) as functions of time for trajectories initialized by distorting the D_{4d} structures (isomer **1**) of the Li_9^+ cluster. For convenience, the corresponding total energies per atom (in eV), shifted by 1 830, and the estimated temperature are also indicated on the right side of the figure[34]

Simulations initialized by energizing the other two higher energy isomers with C_{2v} and C_{3v} structures give rise to substantially different behavior. The graphs of $\langle E_k/n \rangle$ and $\sigma_i(t)$ for the isomer **2** and **3** are shown on Figs 3 and 4. At low excess energy, the fluctuations of atoms are small due to compactness of the C_{2v} and C_{3v} structures, but the isomerization process occurs at an energy (temperature) considerably lower than for trajectories initialized from the D_{4d} form (*cf.* Figs 2–4). Moreover, on the time scale of our simulations the isomerization processes take place from C_{2v} or C_{3v} to D_{4d} form while the inverse process occurs only at energies corresponding to more than 500 K (*cf.* Figs 2–4). In the case of dynamics initiated from the isomer C_{3v}, the isomerization occurs first into the basin of the C_{2v} isomer and than into the basin of the D_{4d} isomer (Fig. 4). This suggests that the activation barriers which control the transition between C_{2v} and C_{3v} are lower than those between C_{2v} and D_{4d} or C_{3v} and D_{4d}. The graphs of $\langle E_k/n \rangle$ exhibit pronounced branches which can be connected with individual isomers (*cf.* graphs 3A and 4A); the $\sigma_i(t)$ quantities provide the same information and in addition also a precise description of the atomistic mechanism of isomerization (*cf.* graphs 3B and 4B).

The bond length fluctuation δ plotted as a function of the cluster energy (see Fig. 5) exhibits two distinct types of energy or temperature dependencies. One (full triangles) is associated with simulations initialized from D_{4d} structure of the isomer **1**, the other (open symbols) has been obtained from trajectories started by distorting the other two isomers lying at higher energies. At relatively low energy a sudden increase in δ value is connected with a mobility of atoms of the centered antiprism which involves a concerted motion of the peripheral atoms, according to analysis based on $\sigma_i(t)$ quantities. Notice that such an increase in δ value at low temperature (excess energy) for the isomer **1** (D_{4d}), is not an indication of a phase transition, which actually occurs at much higher energy (temperature). In fact, the δ value increases very slowly between 200–500 K and then a second abrupt increase occurs due to fast isomerizations involving all three isomers **1**, **2** and **3**.

In contrast, small values of δ are characteristic for the C_{2v} and C_{3v} structures at low temperature (energies) indicating solid-like behavior; the abrupt change for a small increase in energy is due to isomerizations to the D_{4d} form (*cf.* open circles and triangles in Fig. 5). In the range of $T \approx 200$–500 K, in the case of trajectories initialized from configurations related to the isomers C_{2v} and C_{3v}, the values of δ lie above the (almost constant) δ values which characterize the trajectories initialized from the D_{4d} form. The details may change in longer simulations.

The above analysis shows that the lowest energy isomer of Li_9^+, the centered antiprism (D_{4d}), exhibits very different dynamical behavior with increasing energy (temperature) than other two C_{2v} and C_{3v} isomers. All peripheral atoms of the D_{4d} structure perform concerted motion, but remain confined to the energy basin of the equilibrium structure and do not easily rearrange in other isomeric forms until a considerably high

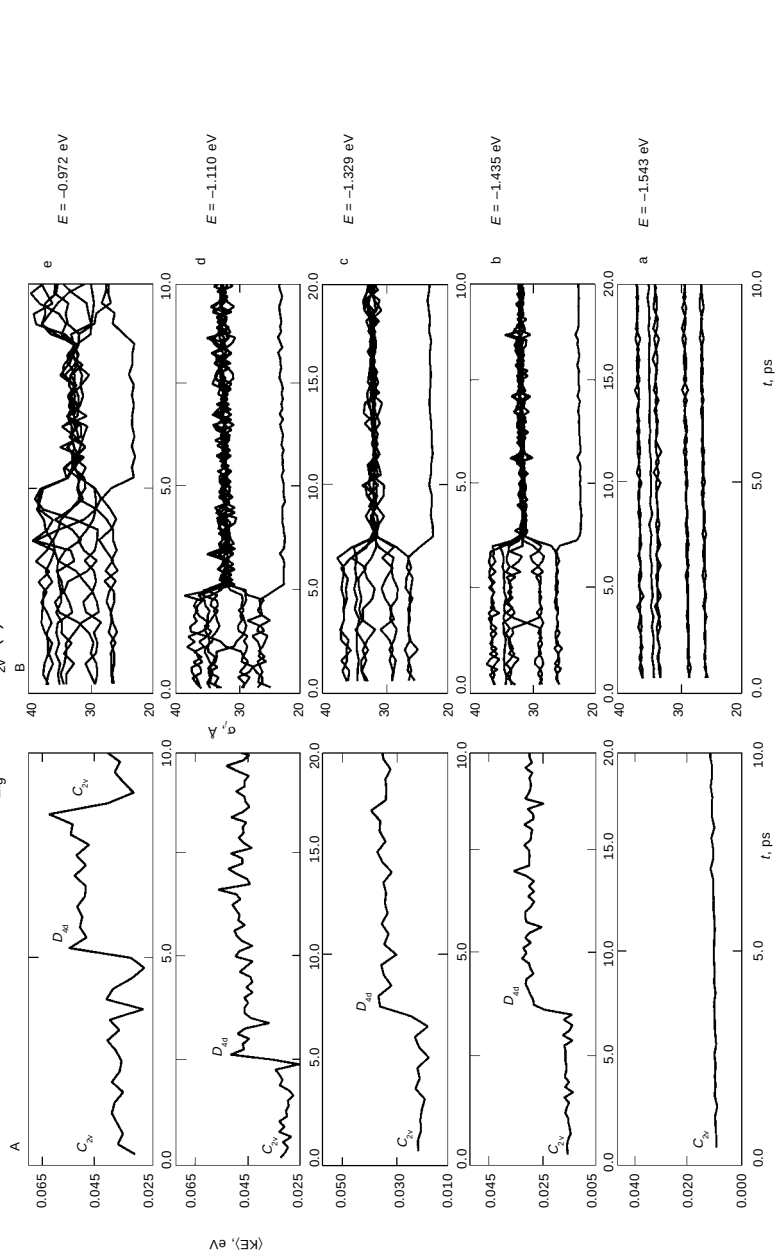

FIG. 3
Short-time (0.25 ps) averaged kinetic energy per atom $\langle KE \rangle$ (A) and "atomic equivalence indexes" $\sigma_i(t)$ (B) as functions of time for trajectories initialized by distorting the C_{2v} structures (isomer **2**) of the Li_9^+ cluster. For convenience, the corresponding total energies per atom (in eV), shifted by 1 830, are also indicated on the right side of the figure[34]

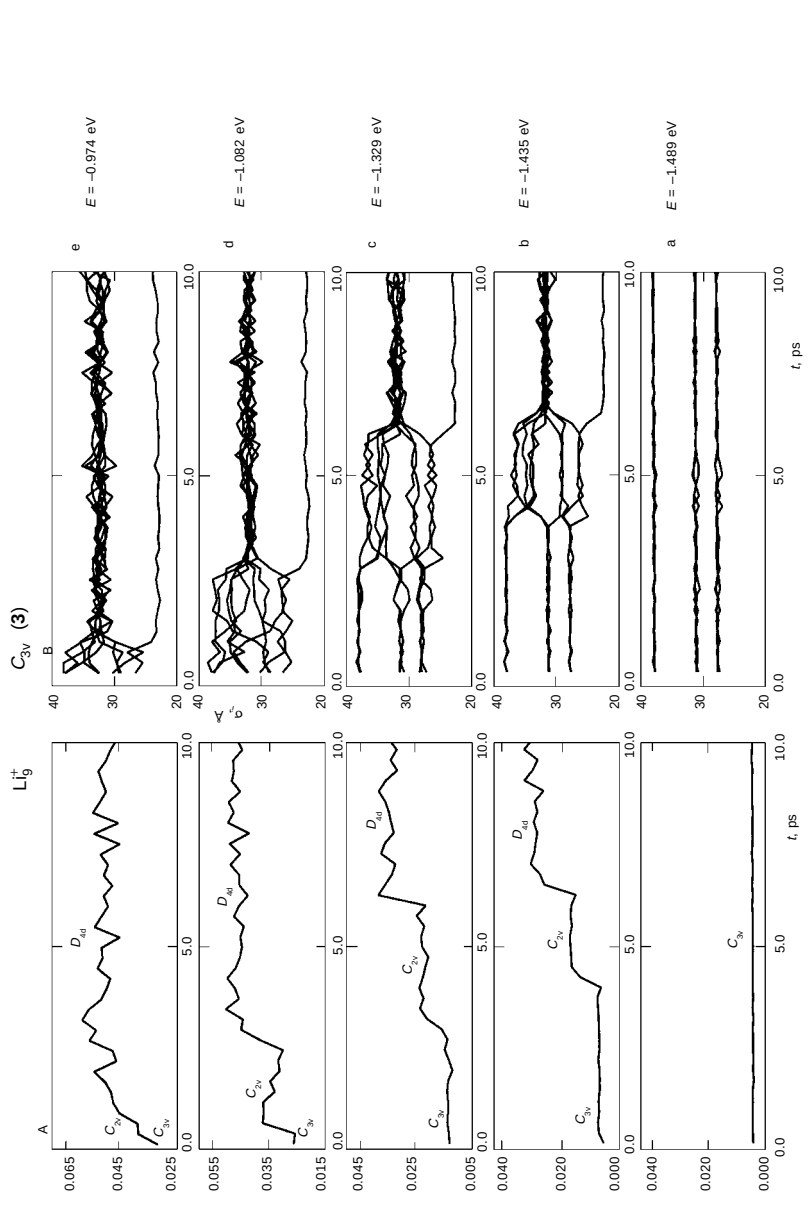

FIG. 4
Short-time (0.25 ps) averaged kinetic energy per atom ⟨KE⟩ (A) and "atomic equivalence indexes" $\sigma_i(t)$ (B) as functions of time for trajectories initialized by distorting the C_{3v} structures (isomer **3**) of the Li_9^+ cluster. For convenience, the corresponding total energies per atom (in eV), shifted by 1 830, are also indicated on the right side of the figure[34]

temperature ($T \approx 500$ K) is reached. Just opposite is the case for the C_{2v} and C_{3v} structures, which exhibit a solid-like behavior at low excess of internal energy but undergo isomerizations already at relatively low temperature ($T \approx 150$ K).

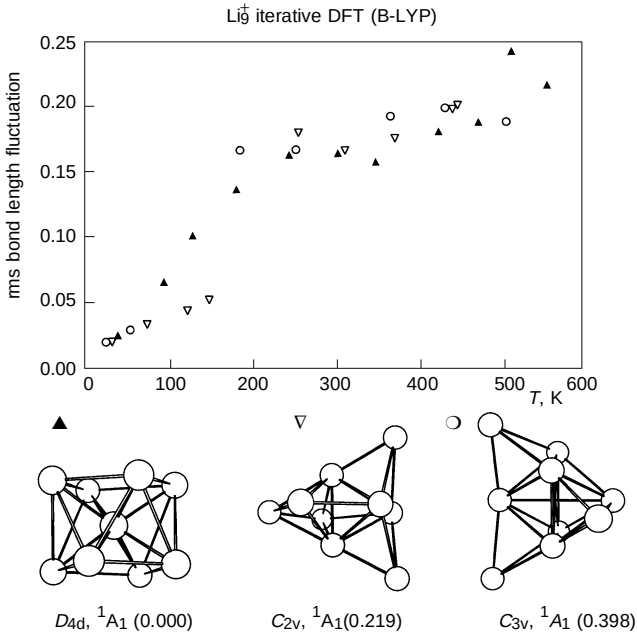

FIG. 5

Root-mean-square bond length fluctuations δ as a function of the total energy. The full and open symbols correspond to trajectories initialized from the D_{4d} and C_{2v}, C_{3v} structures of the isomers **1** (▲), **2** (∇) and **3** (❍), respectively, of Li_9^+ drawn with symmetry labels and energy sequence in eV (ref.[34])

CONCLUSIONS AND OUTLOOK

From investigating the dynamics of different isomeric forms of Li_9^+ the following conclusions can be drawn:

1. A large increase of bond length fluctuation δ does not necessarily indicate a solid-like to liquid-like transition. Therefore the averaged quantity δ must be used with caution to discuss the dynamics of finite size systems, in particularly the alkali metal clusters.

2. The atomic equivalence indexes $\sigma_i(t)$ which contain inherently structural information are well suited to follow dynamical processes along a given trajectory. They proved to be very valuable for determining the atomistic mechanism of isomerization, as it has been illustrated on the example of centered antiprism of Li_9^+. The σ_i values allow to identify transformations leading to equivalent isomeric forms at low excess

energy as well as to follow the multimodal behavior which is characteristic for transition between distinct isomers, at higher excess energies.

3. The individual isomers are characterized by specific dynamic properties as function of different energy. At low excess energy the structures with a central atom exhibit a particular kind of concerted mobility of the peripheral atoms coordinated with the central one, while in C_{2v} or C_{3v} forms atoms undergo only small fluctuations around equilibrium structures. At higher excess energies the latter forms undergo easier isomerization than the former ones.

As mentioned above, the most stable isomer of Na_9^+ assumes the C_{2v} structure: on the basis of our results on Li_9^+ it is possible to estimate that the isomerization process of Na_9^+ occurs at lower temperature (between 200 and 300 K) than for Li_9^+.

4. The higher energy isomers show tendency toward mutual isomerization at lower excess energy (temperatures) due to low activation barriers. Of course, also the activation energy for transformation of less stable isomers to the most stable form is lower than that for the opposite process. This explains why the most stable form exists, without undergoing isomerization, for relatively long times in trajectories characterized by moderate or even high excess energy. This suggests that the basin of the lowest energy isomers might be easier accessed than the basins of other isomers.

From the above described results as well as from our previous AIMD studies an Li_8, Li_{10} and Li_{11}^+ clusters[26] it becomes clear that isomerization processes can take place for different cluster sizes at different temperature, depending on the type of structure of the most stable isomer.

In other words, specific structural properties of clusters must be taken into account, also in the case of systems characterized by large atomic mobility, such as alkali metal clusters.

The analysis of the dynamics of Li_9^+ clearly illustrates that the theoretical approaches explicitly considering the coupling between degrees of freedom of electrons and nuclei are useful tools for a detailed investigation of cluster properties. The development of new methods oriented to the study of time-dependent phenomena involving electronic excitation and motion of nuclei[36] might become an attractive future direction of quantum theory of clusters.

This work has been supported by the Deutsche Forschungsgemeinschaft (SFB 337, Energy transfer in molecular aggregates) and the Consiglio Nationale delle Ricerche (CNR, Rome).

REFERENCES

1. Alivisatos A. P.: *Science* **1996**, *271*, 920.
2. de Heer W., Selby K., Kresin V., Masui J., Vollmer M., Chatelain A., Knight W. D: *Phys. Rev. Lett.* **1987**, *59*, 1805.
3. Alivisatos A. P.: *Science* **1996**, *271*, 933.

4. Pascual J. I., Mendez J., Gomez-Herrero J., Baro A. M., Garcia N., Landmann U., Luedtke W. D., Bogachek E. N., Cheng H.-P.: *J. Vac. Sci. Technol. B* **1995**, *13*, 1280.
5. Barnett R. N., Landmann U.: *Nature* **1997**, *387*, 788.
6. Bonacic-Koutecky V., Fantucci P., Koutecky J.: *Chem. Rev.* **1991**, *91*, 1035; and references therein.
7. Bonacic-Koutecky V., Cespiva L., Fantucci P., Fuchs C., Koutecky J., Pittner J.: *Comments Atom. Mol. Phys.* **1995**, *31*, 233; and references therein.
8. Bonacic-Koutecky V., Fantucci P., Koutecky J.: *Encyclopedia of Computational Chemistry* (P. V. R. Schleyer, Ed.). Wiley, New York, in press.
9. Boustani I., Pewestorf W., Bonacic-Koutecky V., Koutecky J.: *Phys. Rev. B: Condens. Matter* **1987**, *35*, 9437.
10. Bonacic-Koutecky V., Gaus J., Guest M. F., Cespiva L., Koutecky J.: *Chem. Phys. Lett.* **1993**, *206*, 528.
11. Bonacic-Koutecky V., Fantucci P., Koutecky J.: *Phys. Rev. B: Condens. Matter* **1988**, *37*, 4369.
12. Bonacic-Koutecky V., Boustani I., Guest M., Koutecky J.: *J. Chem. Phys.* **1988**, *89*, 4861.
13. a) Wang C., Pollack S., Hunter J., Alameddin G., Hoover T., Cameron D., Liu S., Kappes M. M.: *Z. Phys. D* **1991**, *19*, 13; b) Wang C., Pollack S., Dahlseid T., Koretsky G. M., Kappes M. M.: *J. Chem. Phys.* **1992**, *96*, 7931.
14. Broyer M., Dugourd Ph.: *Comments Atom. Mol. Phys.* **1995**, *31*, 183; and references therein.
15. Baumert T., Thalweiser R., Weiss V., Gerber G. in: *Femtosecond Chemistry* (J. Manz and L. Woste, Eds), p. 397. VCH, Weinheim 1995.
16. Ellert C., Schmitt M., Schmidt C., Reinert T., Haberland H.: *Phys. Rev. Lett.* **1995**, *75*, 1731.
17. a) Bonacic-Koutecky V., Kappes M. M., Fantucci P., Koutecky J.: *J. Chem. Phys. Lett.* **1990**, *170*, 26; b) Bonacic-Koutecky V., Pittner J., Scheuch C., Guest M. F., Koutecky J.: *J. Chem. Phys.* **1992**, *96*, 7938; c) Bonacic-Koutecky V., Fantucci P., Fuchs C., Gatti C., Pittner J., Polezzo S.: *Chem. Phys. Lett.* **1993**, *213*, 522.
18. a) Dugourd Ph., Blanc J., Bonacic-Koutecky V., Broyer M., Chevaleyre J., Koutecky J., Pittner J., Wolf J.-P. , Woste L.: *Phys. Rev. Lett.* **1991**, *67*, 2638; b) Blanc J., Bonacic-Koutecky V., Broyer M., Chevaleyre J., Dugourd Ph., Koutecky J., Scheuch C., Wolf J.-P., Woste L.: *J. Chem. Phys.* **1992**, *96*, 1793.
19. Bonacic-Koutecky V., Fantucci P., Koutecky J.: *Springer Ser. Chem. Phys.* **1994**, *52*, 15.
20. Bonacic-Koutecky V., Pittner J., Fuchs C., Fantucci P., Guest M. F., Koutecky J.: *J. Chem. Phys.* **1996**, *104*, 1427.
21. a) Bonacic-Koutecky V., Pittner J., Koutecky J.: *Chem. Phys.* **1996**, *210*, 313; and references therein; b) Bonacic-Koutecky V., Pittner J.: *Chem. Phys.* **1997**, *225*, 173.
22. a) Brechignac C., Cahuzac Ph., Carlier F., Leygnier J.: *Chem. Phys Lett.* **1989**, *164*, 433; b) Brechignac C., Cahuzac Ph., Carlier F., de Frutos, Leygnier J.: *Z. Phys. D: At., Mol. Clusters* **1991**, *19*, 1; c) Brechignac C., Cahuzac Ph., Carlier F., de Frutos, Leygnier J.: *Chem. Phys. Lett.* **1992**, *189*, 28.
23. Fallgren H., Martin T. P.: *Z. Phys. D: At., Mol. Clusters* **1991**, *19*, 81.
24. Jellinek J., Bonacic-Koutecky V., Fantucci P., Wiechert M.: *J. Chem. Phys.* **1994**, *101*, 10092.
25. Fantucci P., Bonacic-Koutecky V., Jellinek J., Wiechert M., Harrison J. R., Guest M. F.: *Chem. Phys. Lett.* **1996**, *250*, 47.
26. Bonacic-Koutecky V., Jellinek J., Wiechert M., Fantucci P.: *J. Chem. Phys.* **1997**, *107*, 6321.
27. Reichardt D., Bonacic-Koutecky V., Fantucci P., Jellinek J.: *Z. Phys. D: At., Mol. Clusters* **1997**, *40*, 486.
28. Reichardt D., Bonacic-Koutecky V., Fantucci P., Jellinek J.: *Chem. Phys. Lett.* **1997**, *279*, 129.

29. a) Car R., Parrinello M.: *Phys. Rev. Lett*. **1985**, *55*, 2471; b) Car R., Parrinello M. in: *Simple Molecular Systems at Very High Density, NATO ASI Series B: Physics* (A. Polian, P. Loubeyrl and N. Boccara, Eds), Vol. 186, p. 455. Plenum Press, New York 1989.
30. Barnett R. N., Landmann U., Nitzan A., Rajagopal G.: *J. Chem. Phys*. **1991**, *94*, 608.
31. Hartke B., Carter E. A.: *J. Chem. Phys*. **1992**, *97*, 6569.
32. Becke A. D.: *Phys. Rev. A: At., Mol., Opt. Phys*. **1988**, *38*, 3098.
33. Lee C., Yang W., Parr R. G.: *Phys. Rev. B: Solid State* **1988**, *37*, 785.
34. Reichardt D., Bonacic-Koutecky V., Fantucci P.: Unpublished results.
35. Rothlisberger U., Andreoni W.: *J. Chem. Phys*. **1991**, *94*, 8129.
36. Hartmann M., Pittner J., Bonacic-Koutecky V., Heidenreich A., Jortner J.: *J. Chem. Phys*. **1998**, *108*, 3096.